Potential Therapeutic Activity of Berberine in Thyroid-Associated Ophthalmopathy: Inhibitory Effects on Tissue Remodeling in Orbital Fibroblasts

Jiale Diao, Xinxin Chen, Pei Mou, Xiaoye Ma, and Ruili Wei

Department of Ophthalmology, Changzheng Hospital of Naval Medicine University, Huangpu District, Shanghai, China

Correspondence: Ruili Wei, Department of Ophthalmology, Changzheng Hospital of Naval Medicine University, 415 Fengyang Road, Huangpu District, Shanghai 200003, China; ruiliwei@smmu.edu.cn.

JD and XC contributed equally to this article and XC is the co-first author.

Received: April 16, 2022
Accepted: August 11, 2022
Published: September 12, 2022

Citation: Diao J, Chen X, Mou P, Ma X, Wei R. Potential therapeutic activity of berberine in thyroid-associated ophthalmopathy: Inhibitory effects on tissue remodeling in orbital fibroblasts. *Invest Ophthalmol Vis Sci.* 2022;63(10):6. https://doi.org/10.1167/iovs.63.10.6

Purpose. Berberine (BBR), an alkaloid produced by a traditional Chinese plant, was recently attributed multiple effects on lipometabolism, inflammation, and fibrosis. Thyroid-associated ophthalmopathy (TAO) is highly associated with these pathologic changes. Thus, we aimed to examine the potential therapeutic effect of BBR in an in vitro model of TAO.

Methods. Orbital fibroblasts (OFs) obtained from control donors ($n = 6$) or patients with TAO ($n = 6$) were cultured. The CCK-8 assay was conducted for assessing the optimal concentration range. Oil Red O staining, Western blotting, and quantitative RT-PCR (qRT-PCR) were conducted to assess adipogenesis in OFs. RNA sequencing (RNA-seq) was used to screen the key pathways of the antiadipogenic effect mediated by BBR. Along with incremental concentrations of BBR, IL-1β–induced expression of proinflammatory molecules was determined by ELISA and qRT-PCR. In addition, TGF-β–induced hyaluronan (HA) production and fibrosis were evaluated by ELISA, qRT-PCR, and Western blotting.

Results. TAO-OFs, but not control fibroblasts (CON-OFs), were readily differentiated into adipocytes with the commercial medium. Intracellular lipid accumulation was dose-dependently decreased by BBR, and adipogenic markers were also downregulated. Moreover, the PPARγ and AMPK pathways were screened out by RNA-seq and their downstream effectors were suppressed by BBR. Besides, BBR attenuated IL-1β–induced expression of proinflammatory molecules in both TAO-OFs and CON-OFs by blocking nuclear factor–κB signaling. BBR's inhibitory effect on TGF-β–mediated tissue remodeling was also confirmed in OFs.

Conclusions. These findings demonstrate BBR has outstanding capabilities of controlling adipogenesis, inflammation, HA production, and fibrosis in OFs, highlighting its potential therapeutic role in TAO management.

Keywords: thyroid-associated ophthalmopathy, berberine, orbital fibroblast, adipogenesis, fibrosis

Thyroid-associated ophthalmopathy (TAO), or Graves' ophthalmopathy, represents an autoimmune orbital disorder with diverse clinical manifestations. Most patients simultaneously have several symptoms but in different patterns, including lid retraction, ocular aching, exophthalmos, and restricted strabismus. Severe cases, representing 3% to 5% of all patients, may develop a sight-threatening condition with refractory corneal lesion or optic neuropathy.[1,2] Underlying these features, orbital fibroblasts (OFs) act as key players and are responsible for the unique manner of tissue remodeling and inflammatory reactions in the TAO orbit. Autoimmune cell infiltration and thyrotropin receptor (TSHR)/insulin-like growth factor 1 receptor (IGF-IR) activation induce OFs to cause excessive adipogenesis, glycosaminoglycan production, and inflammatory cascade.[3,4] Multiple inflammatory factors secreted by OFs, including IL-1β, IL-6, and COX-2, in turn enhance autoimmune and inflammatory reactions.[5,6] Moreover, hyaluronan (HA) accumulation can also be stimulated by TGF-β,[7] which induces myodifferentiation in OFs and fibrosis in extraocular muscles.[8] Thus, OFs are considered the core of TAO pathogenesis research and the prime target for novel pharmaceuticals.[9]

Pulse therapy with high-dose glucocorticoids (GCs) remains a traditional management in active, moderate to severe TAO cases. However, owing to its well-known side effects and limitations,[10] GCs can only be used under comprehensive monitoring and control. For GC-resistant/contraindicated TAO, a wide range of studies developing targeted biological agents and small-molecular inhibitors have been performed in past decade. Biological therapies like rituximab (targeting CD20) and tocilizumab (IL-6 receptor antagonist) have satisfactory improvement in clinical activity score (CAS) but no confirmed effects on proptosis or strabismus and have relatively high rates of adverse events.[11,12] Teprotumumab (anti–IGF-IR antibody) emerges as the first approved medicine for TAO in United States, which has high response rates with significant

improvements in proptosis, CAS, and diplopia; long available duration; and mild side effects.[13,14] Nevertheless, monoclonal antibodies, even teprotumumab, bear high costs and still available in a few regions, which may impose a burden on most patients with TAO. Therefore, more economically affordable drugs are essential for TAO therapy.

Berberine (BBR), formula $C_{20}H_{18}NO_4$, represents the primary bioactive component of *Rhizoma coptidis* (known as "Huang Lian" in Chinese), which has diverse pharmacologic activities. At the early stage of its development, BBR was widely used as a safe and effective drug for treating bacterial gastroenteritis and diarrhea.[15] In recent studies, BBR was demonstrated to decrease lipid amounts in 3T3-L1 adipocytes, foam cells, and hepatocytes.[16–18] Furthermore, BBR is considered by several scholars a nutraceutical for lipid lowering.[19] On the other hand, evidence shows the anti-inflammatory effects of BBR, decreasing proinflammatory cytokines/mediators, are pervasively substantial in cardiomyocytes, vascular endotheliocytes, and hepatocytes. BBR also restrains collagen production and myofibroblast transformation into cardiac fibroblasts.[20]

Given the abovementioned bioactivities, BBR could have a potential therapeutic activity in TAO. In this report, we first explored its antiadipogenic effect and explored the underlying mechanisms in TAO OFs. We demonstrated inflammation, HA production, and fibrosis-related processes can also be alleviated by BBR treatment in OFs.

Materials and Methods

Berberine (CSN13524) was purchased from CSNpharm (Chicago, IL, USA) and dissolved with dimethyl sulfoxide (DMSO) in 10 mM for storage solution. High-glucose Dulbecco's modified Eagle's medium (DMEM), fetal bovine serum (FBS), 0.25% trypsin-EDTA, and human IL-1β recombinant protein (PHC0815) were provided by Gibco (Waltham, MA, USA). Mesenchymal stem cell adipogenic differentiation medium (DM) was obtained from ScienCell (Carlsbad, CA, USA). Phosphate-buffered saline (PBS), Modified Oil Red O Staining Kit (C0158S), DMSO, 4% paraformaldehyde (PFA), and penicillin/streptomycin solution (100×) were acquired from Beyotime (Shanghai, China). TRIzol reagent and RNA-Quick Purification Kit (RN001) were purchased from Invitrogen (Carlsbad, CA, USA) and Shanghai Yishan Biotechnology (Shanghai, China), respectively. Recombinant human TGF-β1 (AF-100-21C) and Fast Western blot kit, ECL Substrate (35050) were provided by PeproTech (Rocky Hill, NJ, USA) and Pierce (Rockford, IL, USA), respectively. The PAGE Gel Fast Preparation Kit was provided by EpiZyme (Shanghai, China). PrimeScript RT Master Mix (RR036A) and TB Green Premix Ex Taq (RR420A) reagent kits were obtained from Takara (Otsu, Japan). Cell Counting Kit 8 (CCK-8) was provided by DOJINDO (Kumamoto, Japan).

Patients, Sample Collection, and Cell Cultures

Orbital adipose specimens were collected from inactive, moderate to severe TAO cases ($n = 6$) during orbital decompression. All patients with TAO were euthyroid, were CAS <3, had absence of compressive optic neuropathy, and received no GCs, immunosuppressors, or external beam radiation for over 6 months prior to decompression. Healthy donors were patients who underwent cosmetic surgeries ($n = 6$). Control fibroblasts (CON-OFs) were cultured using central fat under the orbital septum. Those cases had no TAO or other immunologic thyroid diseases according to their annually medical examination reports and medical histories. All surgeries were conducted at the Department of Ophthalmology, Changzheng Hospital, Shanghai, China. Detailed information of patients is presented in the Table, and medication history of prostaglandin analogues was mentioned, as it has been reported that they can affect many pathways studied.[21] This research was approved by the Committee on Ethics of Biomedicine, Naval Medical University. Each sampled specimen and signed informed consent were acquired according to the 1964 Declaration of Helsinki.

OFs were cultured based on a published protocol.[22] Concisely, orbital adipose tissues were minced mechanically into 1-mm^3 pieces and placed in culture dishes. After adherence, explants were soaked into high-glucose DMEM supplemented with 20% FBS and 1% penicillin/streptomycin. OFs generally migrate from explants in about 3 days and reach confluence in 10 days. The passage of monolayer cells was carried out with 0.25% trypsin/EDTA to establish a cell line. To ensure the efficiency of differentiation, cells of low passage (three to four passages) were used in adipogenesis experiments while five to eight passage cells were utilized

Table. Detailed Information of the Donors Recruited in the Study

Age, y/Sex	Duration of TAO, y	Proptosis (R/L), mm	Smoking	CAS	Previous TAO Treatment	Thyroid Treatment	Prostaglandin Analogues	Surgical Treatment
Patients with TAO								
33/M	2.4	21/22	Previous	2/7	GC	Methimazole	None	Orbital decompression
46/F	7.8	18/18	No	0/7	None	No	None	Orbital decompression
38/M	6	24/19	Previous	1/7	GC	No	None	Orbital decompression
57/F	12	19/20	No	0/7	GC	Thyroidectomy	None	Orbital decompression
53/F	7.4	17/19	No	0/7	GC	RAI, thyroidectomy	None	Orbital decompression
26/F	1.6	21/23	No	2/7	None	Methimazole	None	Orbital decompression
Control patients								
40/F	—	—	No	—	—	—	None	Upper lid blepharoplasty
39/M	—	—	Yes	—	—	—	None	Eyelid pouch plasty
27/F	—	—	No	—	—	—	None	Upper lid blepharoplasty
33/F	—	—	No	—	—	—	None	Upper lid blepharoplasty
46/F	—	—	Previous	—	—	—	None	Eyelid pouch plasty
29/F	—	—	No	—	—	—	None	Upper lid blepharoplasty

CAS is a total of 7 points. F, female; L, left; M, male; R, right; RAI, radioactive iodine.

Investigative Ophthalmology & Visual Science

for other assays. At least three independent OF lines were used in each experiment.

Adipogenesis

OFs were seeded in 6-well or 12-well plates at 10,000/cm^2. At 100% confluence, the standard medium was switched to DM or proliferation medium (PM). The base medium of PM was high-glucose DMEM. The proportion of FBS in PM was 5%, matching the concentration of DM. According to the manufacturer's instructions, the medium was substituted with fresh DM every 4 to 5 days. The induction was sustained for approximately 20 days along with BBR (0.1, 0.5, or 1 µM). Differentiated OFs underwent fixation with 4% PFA and staining with Oil Red O solution. Furthermore, OFs were lysed for RNA extraction after 5-day and 10-day induction, while Western blot was conducted with 12-day differentiated OFs.

Oil Red O Staining

Oil Red O staining was implemented with the Modified Oil Red O Staining Kit, as directed by the manufacturer. In brief, the OF monolayer underwent soft washing with PBS twice and fixation with 4% PFA (15 minutes) at ambient temperature. Upon rinsing with the staining detergent, cells underwent incubation with modified Oil Red O solution at 37°C for 30 minutes. OFs after staining were inspected and photographed with a phase-contrast microscope (Olympus CKX41; Olympus, Tokyo, Japan). Besides using analytical-grade isopropanol, staining was extracted for the quantification of lipids. Absorbance was read on a SpectraMax i3x Multi-Mode Microplate Detection Platform (Molecular Devices, San Jose, CA, USA) at 490 nm.

Cytotoxicity Assay

CCK-8 was adopted to assess cellular viability. OFs underwent seeding into a 96-well plate at 5×10^3/well in standard medium with or without BBR treatment. Cell culture supernatant containing CCK-8 reagent was assessed with the abovementioned microplate reader for OD values at 450 nm. All experiments were conducted in line with the manufacturer's instructions.

RNA Sequencing Analysis

The BGISEQ platform was utilized for transcriptome sequencing in nine cell samples, including the PM, DM, and BBR (1 µM) groups ($n = 3$). The samples were cultured for 5 days in indicated conditions and subsequently lysed with TRIzol reagent. Differentially expressed genes (DEGs) in pairwise comparisons were identified with a Q-value <0.05 and $|\log2FC| > 1$. Pathway enrichment for DEGs was obtained through the Kyoto Encyclopedia of Genes and Genomes (KEGG) Pathway database.

ELISA

Conditioned supernatants were taken from the cell culture medium and stored at −80°C for subsequent examination. Secreted HA, IL-6, pentraxin 3 (PTX3), and cyclooxygenase-2 (COX-2) amounts were detected with commercial ELISA kits (HA, R&D Systems, Minneapolis, MN, USA; IL-6, PTX3 and COX-2, Elabscience Biotechnology, Wuhan, China), as directed by the respective manufacturers. Triplicate assays were carried out.

Western Blot Assay

As described previously, Western blot was implemented in a standard manner.[23] Primary antibodies are listed in Supplementary Table S1. Each band was converted to image intensity and assessed by the ImageJ software (National Institutes of Health, Bethesda, MD, USA). β-Actin or glyceraldehyde-3-phosphate dehydrogenase (GAPDH) was utilized for normalization in different experiments.

Quantitative RT-PCR

Total RNA isolation utilized the RNA-Quick Purification Kit according to the manufacturer's instructions. RNA concentration and purity were assessed on a Nanodrop 2000 (Thermo Fisher, Waltham, MA, USA). Reverse transcription and quantitative RT-PCR (qRT-PCR) were conducted with Takara reagent kits on an ABI Prism 7900HT system.[24] In addition, GAPDH or β-Actin was utilized for normalization in different experimental conditions due to the probably unstable expression of GAPDH in adipogenesis and IL-1β induction.[25] The primers of target genes are presented in Supplementary Table S2.

Statistical Analysis

All statistical analyses were conducted with GraphPad Prism v9.3 (GraphPad Software, La Jolla, CA, USA). Data are mean ± SD from at least three different OF lines, examined in triplicate. One-way ANOVA was carried out for significance analysis in different treatments, and two-way ANOVA was conducted between TAO-OFs and CON-OFs. $P < 0.05$ indicated statistical significance.

Results

Suppressive Effects of BBR on Adipogenesis in TAO-OFs

Despite the relatively high safety of BBR,[26] the CCK-8 assay was conducted in OFs to confirm the noncytotoxic concentrations. As shown in Supplementary Figure S1, BBR was noncytotoxic until a concentration of >20 µM, and these trends were consistent in TAO-OFs and CON-OFs at indicated times. To completely exclude potential errors caused by cytotoxicity, we used BBR at concentrations of <10 µM for subsequent investigation. In addition, in consideration of the lengthy adipogenic duration and low adhesion of adipocytes, the concentration of BBR was further decreased according to our preliminary experiments.

OFs were cultured under adipogenic differentiation conditions for 20 days followed by Oil Red O staining. As demonstrated in Figures 1A and 1B, DM induced lipid droplet formation (6.0-fold) in TAO-OFs, and this effect was dose-dependently suppressed (6.0-fold vs. 4.8-, 2.9-, and 1.4-fold) by BBR. This induction was not found in CON-OFs, with no significant difference among the PM, DM, and BBR groups. The relative absorbances of TAO-OFs were higher than those of CON-OFs in DM and BBR (0.1 and 0.5 µM) groups (two-way ANOVA, all $P < 0.01$). Triplicate images are presented in Supplementary Figures S2 and S3.

Investigative Ophthalmology & Visual Science

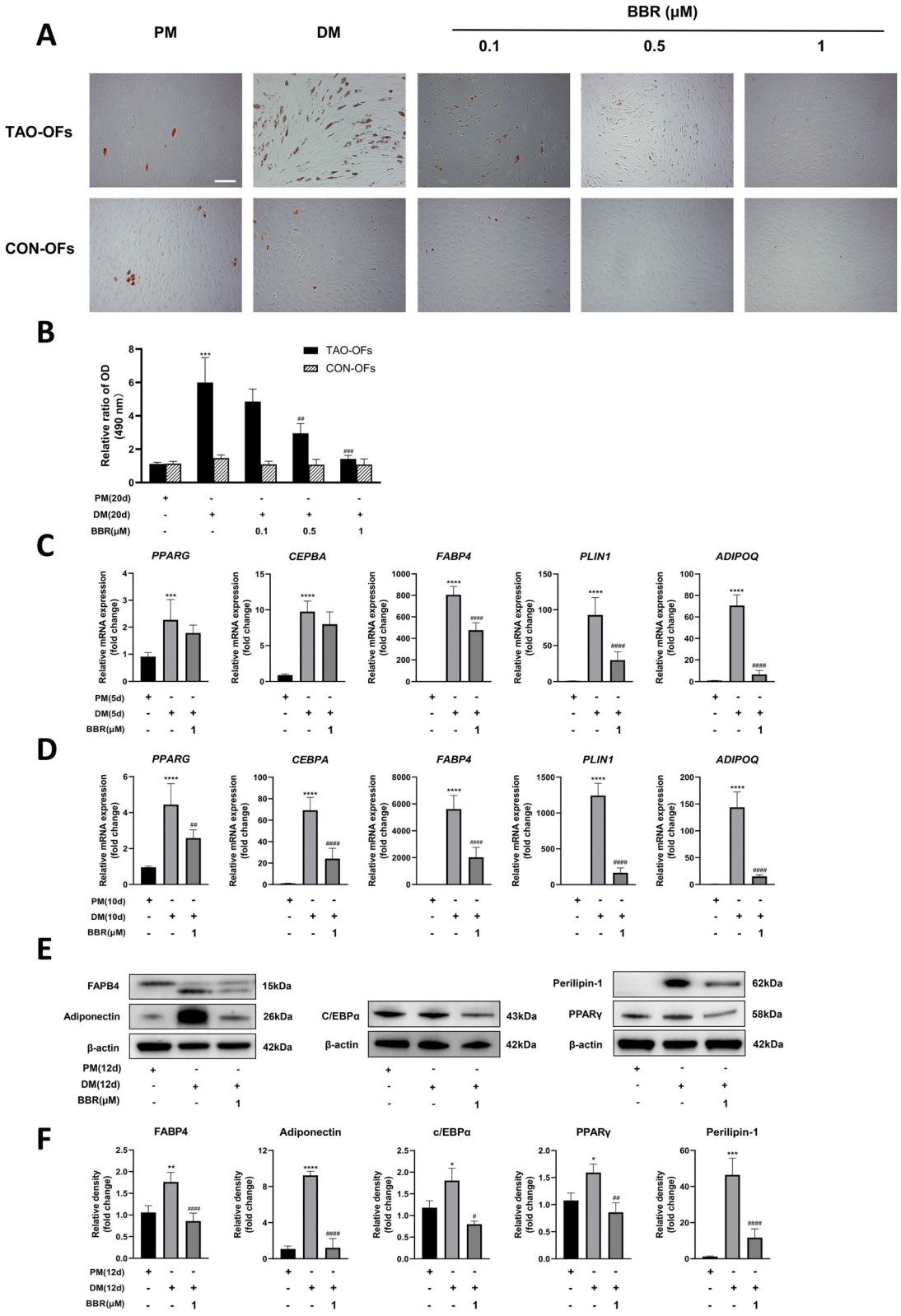

Figure 1. Suppressive effects of BBR on adipogenesis in TAO-OFs. (**A**) Intracellular fat accumulation displayed by Oil Red O staining with or without incremental treatment concentrations of BBR (0.1, 0.5, and 1 μM) in TAO-OFs and CON-OFs. The morphologic characteristics of OFs were observed under a microscope (100×). Scale bar: 100 μm. (**B**) Staining levels were relatively quantified by detecting OD values at 490 nm, $n = 3$. (**C**, **D**) After 5 and 10 days of differentiation with or without BBR (1 μM), the mRNA levels of *PPARG*, *CEBPA*, *FABP4*, *PLIN1*, and *ADIPOQ* were determined, $n = 6$. (**E**) After 12 days of adipogenesis with or without BBR (1 μM), the protein levels of the corresponding markers were examined. (**F**) The bands of indicated proteins were quantified by densitometry, $n = 3$. Relative quantification was normalized to β-actin. $^{*}P < 0.05$, $^{**}P < 0.01$, $^{***}P < 0.001$ and $^{****}P < 0.0001$ versus control group; $^{\#}P < 0.05$, $^{\#\#}P < 0.01$, $^{\#\#\#}P < 0.001$, and $^{\#\#\#\#}P < 0.0001$ versus DM group, one-way ANOVA.

Investigative Ophthalmology & Visual Science

Further, several transcription factors were pivotal for adipocyte maturation.[27] *PPARG*, *CEBPA*, *FABP4*, *PLIN1*, and *ADIPOQ* mRNA expression were significantly elevated (~2.3- to 5618-fold) in the DM group after 5- and 10-day induction (Figs. 1C, 1D). BBR curbed the upregulation of adipogenic markers in both mRNA and protein levels (Figs. 1E, 1F). Interestingly, we found *CEBPA* and *PPARG* were not significantly suppressed by BBR until 10 days later, while *FABP4*, *PLIN1*, and *ADIPOQ* were repressed from the beginning. CON-OFs were excluded due to the poor adipogenic capacity.

PPARγ and AMPK Pathways Participate in BBR-Mediated Antiadipogenic Effect

To investigate the potential mechanism by which BBR represses adipogenesis, RNA sequencing (RNA-seq) was utilized to determine the gene expression profile of TAO-OFs with various treatments. Pearson correlation analysis, as a quality control test, was performed (Fig. 2A). Through precise bioinformatics analysis, we identified total DEGs in PM-versus-DM and DM-versus-BBR, which were shaped in volcano plots (Figs. 2B, 2C). Furthermore, we narrowed the range of DEGs and relevant transcripts based on the fold-change threshold (Figs. 2D, 2G). As shown in Venn diagrams (Figs. 2E, 2H), 853 DEGs and 2140 transcripts were upregulated in PM-versus-DM, while 374 DEGs and 1103 transcripts were downregulated in DM-versus-BBR. Among them, 99 DEGs and 254 transcripts, respectively, were selected as the targets to obtain KEGG pathway enrichment.

As demonstrated in Figures 2F and 2I, the PPARγ and AMPK signaling pathways topped the list. PPARγ pathway blockage is demonstrated in Figure 1E. Considering the BBR's capacity to activate AMPK signaling in multiple metabolic studies,[28–30] AMPK's role in the antiadipogenic effect of BBR was examined. Unexpectedly, AMPK phosphorylation was not elevated but significantly decreased in TAO-OFs after BBR treatment (Figs. 2J, 2M), yet the expression of downstream proteins (SREBP1, SCD1) was promoted by DM and downregulated by BBR (Figs. 2K, 2L and 2N, 2O). These findings were partially consistent with RNA-seq results and indicated AMPK pathway and PPARγ pathway inhibition were both found in BBR-induced antiadipogenesis.

BBR Suppresses IL-1β–Induced Inflammation

Orbital inflammation has been demonstrated to play a crucial role in TAO pathogenesis.[31] Thus, qRT-PCR and ELISA were conducted to determine the effect of BBR on proinflammatory molecules stimulated by IL-1β. As depicted in Figure 3, mRNA amounts of *IL-6*, *PTX3*, *COX-2*, and *IL-1β* were elevated (~29- to 2369-fold) by IL-1β, and BBR treatment dose-dependently suppressed these increases. Among these, the levels of *IL-6* and *COX-2* in all groups and PTX3 in the IL-1β–treated group were higher (two-way ANOVA, all $P < 0.05$), although *IL-1β* itself was lower (two-way ANOVA, $P = 0.0005$) in TAO-OFs. The BBR-induced trends of protein levels in culture supernatants conformed to the above mRNA results (Figs. 3E–G). However, the baseline concentrations of PTX3 and COX-2 were higher in TAO-OFs, in contrast to IL-6 (two-way ANOVA, all $P < 0.0001$). IL-1β was not included due to the extrinsic interference.

Furthermore, IL-1β induces the production of proinflammatory molecules through the nuclear factor (NF)–κB signaling pathway.[32] To assess BBR's role in this pathway, the protein level of NF-κB p65 was determined. Interestingly, NF-κB was induced by IL-1β only in TAO-OFs, and BBR cotreatment downregulated this activation (Figs. 3H, I).

BBR Inhibits HA Production and Fibrosis Induced by TGF-β

The involvement of extraocular muscles in TAO pathogenesis is based on excessive HA accumulation[7] and subsequent fibrosis with a stable duration, which are both boosted by TGF-β.[33] Accordingly, we first performed ELISA and qRT-PCR to clarify whether BBR suppressed HA biosynthesis and hyaluronan synthase (*HAS1*, *HAS2*, and *HAS3*) gene expression. As shown in Figure 4A, TGF-β1 promoted HA production in OFs, which was substantially decreased by BBR treatment. No difference showed in HA concentration between TAO-OFs and CON-OFs in all groups (two-way ANOVA, all $P > 0.05$). However, *HAS1* mRNA expression changes were higher (two-way ANOVA, all $P < 0.0001$ except BBR 10-µM group) in TAO-OFs, while *HAS2* and *HAS3* were higher (two-way ANOVA, all $P < 0.0001$) in CON-OFs.

The degree of fibrosis can be measured as the mRNA and protein levels of related fibrotic core markers (*ACTA2*, *FN1*, *COL1A1*, and *COL3A1*). Incubation with TGF-β1 increased the mRNA levels of fibrotic markers, and BBR had dose-dependent inhibitory effects on these genes (Fig. 4B). Regardless of treatments, the level of *ACTA2* was higher in CON-OFs, while *FN1* was lower (two-way ANOVA, all $P < 0.001$). *COL1A1* and *COL3A1* in TAO TGF-β–treated groups were higher (two-way ANOVA, all $P < 0.001$). The protein expression levels determined by Western blot also confirmed the antifibrotic effect of BBR (Figs. 4C–E).

Discussion

As a major ingredient of a classical Chinese herb, berberine has recently attracted much more attention for its various therapeutic effects in multiple diseases, including fibrosis-related pathologies, cancer, and cardiovascular and metabolic disorders.[28,34,35] According to recent studies, BBR exerts the above pharmacologic effects by regulating inflammation, oxidative stress, apoptosis, fibrosis, and glucose and lipid metabolism, probably covering a large part of TAO pathogenesis. Additionally, increasingly more studies have demonstrated the safety of BBR at conventional doses,[26,36] which makes its clinical transformation easier in TAO management compared with other new drugs. Therefore, we first assessed BBR's effects on TAO OFs to reveal its potential therapeutic value.

About two-thirds of TAO cases, mostly under 40 years old and nonsmokers, are characterized by excessive adipogenesis resulting in orbital fat expansion.[37] Our experiments showed that BBR potently attenuated adipogenesis in TAO OFs. Intracellular fat accumulation determined by Oil Red O staining and upregulated adipogenic markers both demonstrated that BBR effectively induces antiadipogenesis. However, CON-OFs differentiating into adipocytes hardly occurred, and statistical significance was not reached, even though BBR seems to thoroughly eliminate the few lipids stained in CON-OFs images (Supplementary Fig. S3). Such results conformed to several studies.[38–40] Further, to elucidate the underlying mechanism of this inhibition, RNA-seq was conducted to screen DEGs and the enriched pathways.

Investigative Ophthalmology & Visual Science

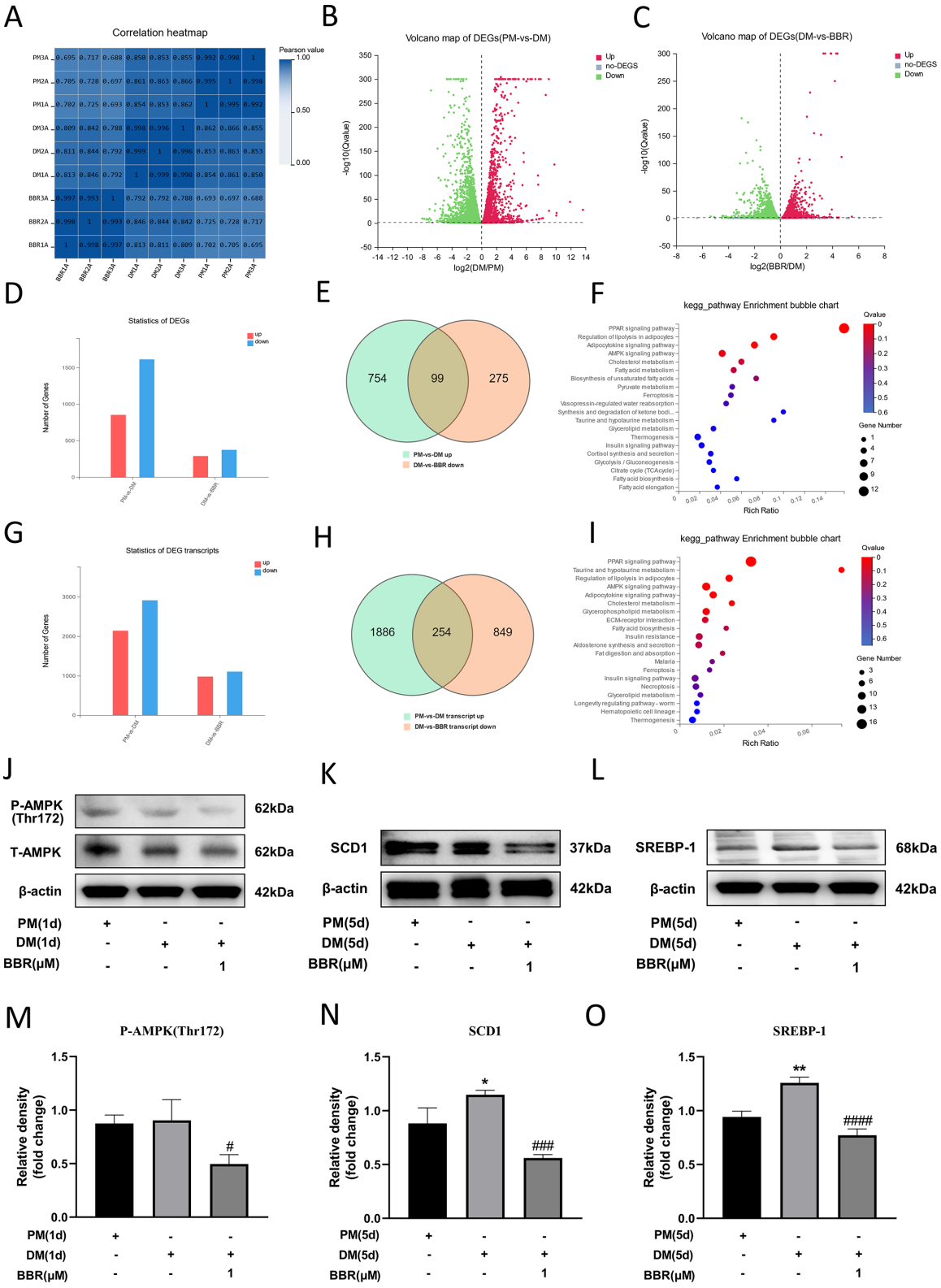

Figure 2. The PPARγ and AMPK pathways participate in a BBR-mediated antiadipogenic effect. (**A**) Pearson correlation analysis of RNA-seq data in the PM, DM, and BBR groups. (**B–D**, **G**) Volcano plots and statistics of DEGs and transcripts for PM versus DM and DM versus BBR. (**E**, **H**) Venn diagrams of DEGs showing 99 genes and 254 transcripts were upregulated by DM and downregulated by BBR, respectively. (**F**, **I**) KEGG pathway enrichment after BBR treatment of DM. (**J**) After 1 day of induction, the protein levels of AMPK and its phosphorylation (Thr172) were assessed. (**K**, **L**) After 5 days of induction, SCD1 and SREBP-1 protein amounts were determined. (**M–O**) Densitometric quantitation of Thr172 normalized to t-AMPK, SCD1 and SREBP-1 normalized to β-actin were calculated ($n = 3$). Relative quantifications were based on β-actin expression. *$P < 0.05$, **$P < 0.01$, ***$P < 0.001$, and ****$P < 0.0001$ versus control group; #$P < 0.05$, ##$P < 0.01$, ###$P < 0.001$, and ####$P < 0.0001$ versus DM group, one-way ANOVA.

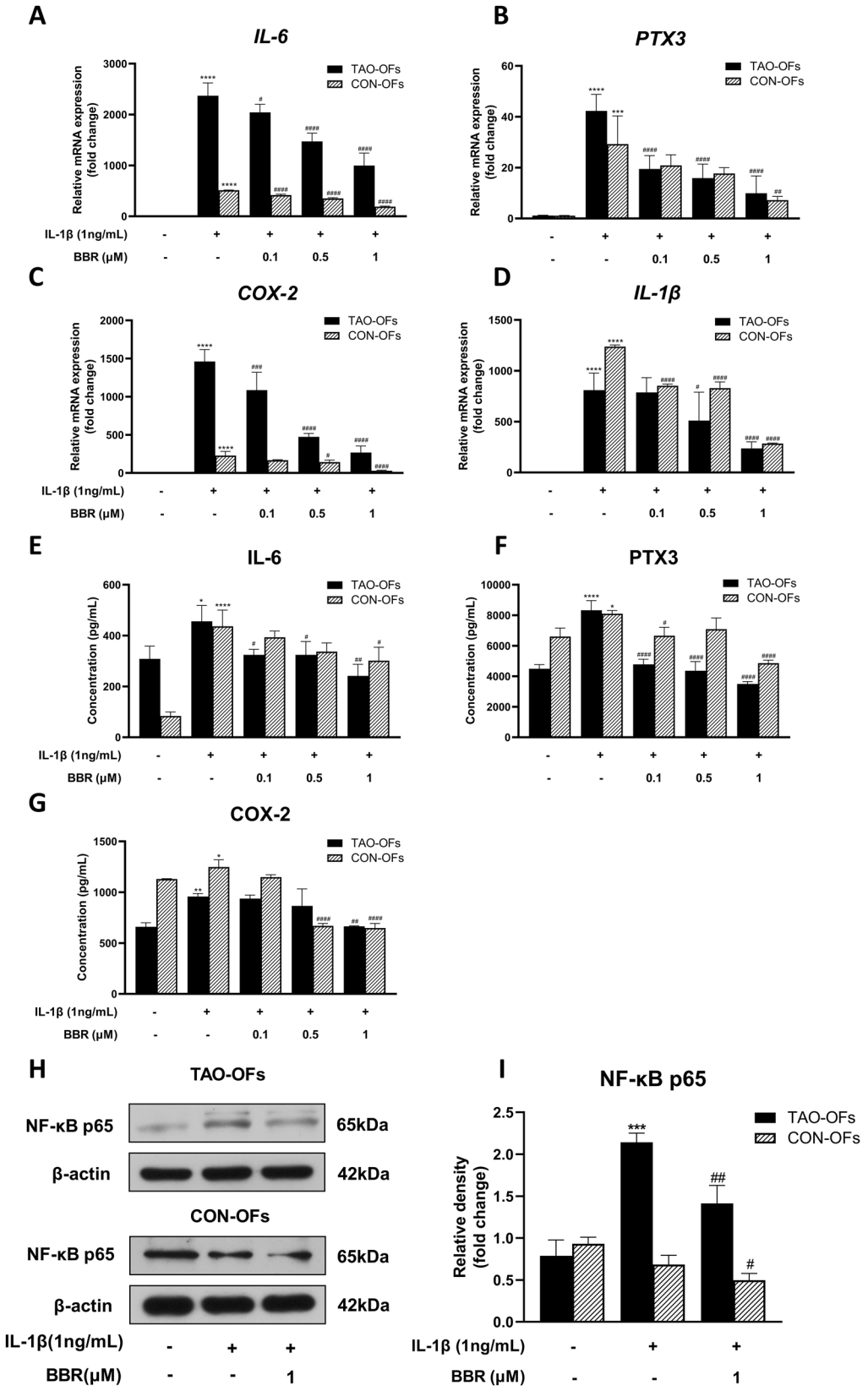

Figure 3. Effect of BBR suppression on IL-1β–associated inflammation. OFs were pretreated with BBR (0, 0.1, 0.5, and 1 μM) for 12 hours and then incubated with IL-1β (1 ng/mL) for another 6 hours. *IL-6* (**A**), *PTX3* (**B**), *COX-2* (**C**), and *IL-1β* (**D**) mRNA amounts were determined ($n = 6$ vs. 3). (**E–G**) The indicated protein concentrations in the supernatants were detected after incubation with IL-1β (1 ng/mL) for another 24 hours ($n = 3$). (**H**) The NF-κB p65 was assessed and quantified upon incubation with IL-1β (1 ng/mL) for another 1 hour. (**I**) Relative quantification was based on β-actin protein amounts ($n = 3$). *$P < 0.05$, **$P < 0.01$, ***$P < 0.001$, and ****$P < 0.0001$ versus control group; #$P < 0.05$, ##$P < 0.01$, ###$P < 0.001$, and ####$P < 0.0001$ versus IL-1β group, one-way ANOVA.

Investigative Ophthalmology & Visual Science

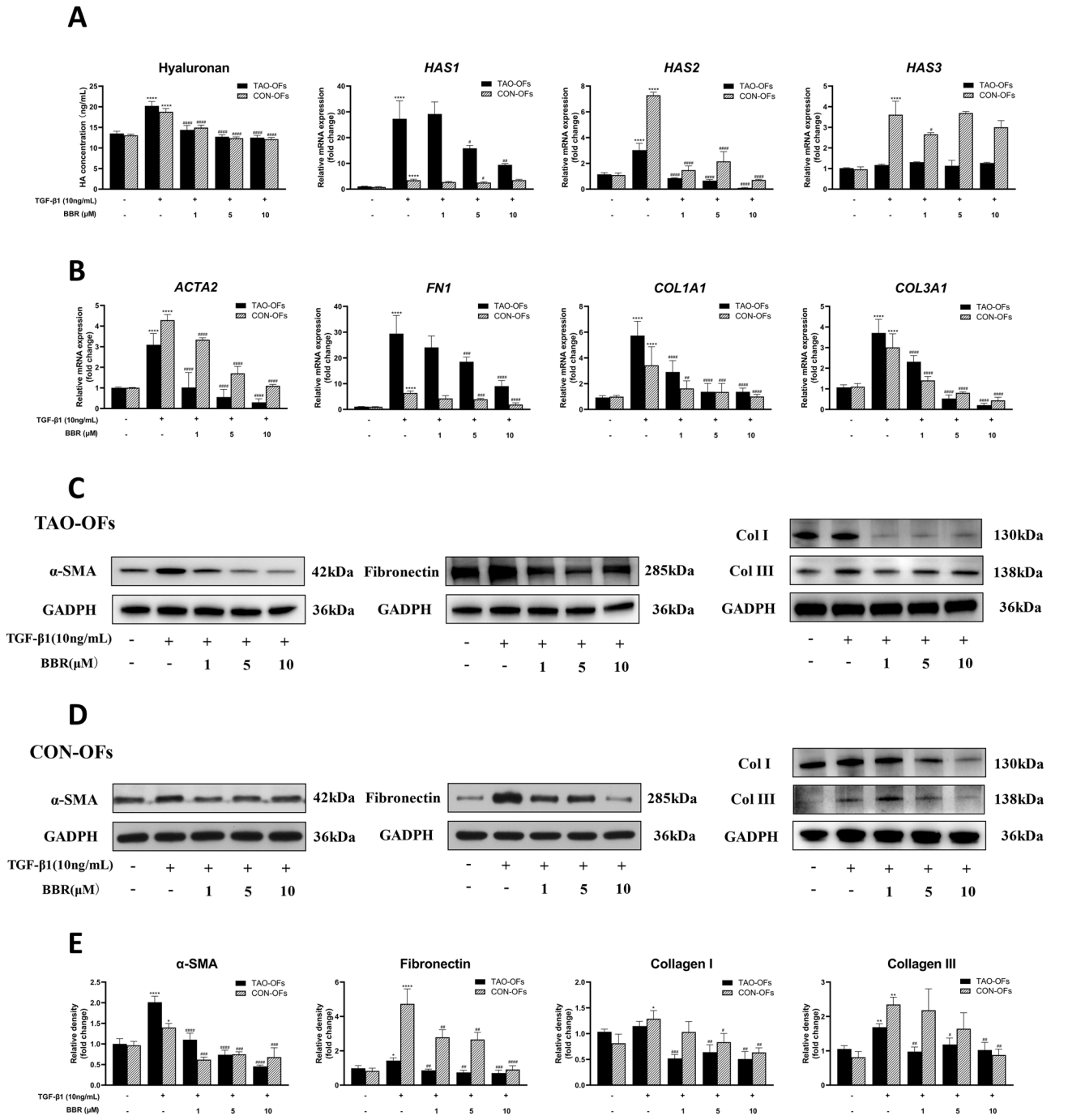

Figure 4. Inhibitory effect of BBR on HA production and fibrosis induced by TGF-β. (**A**) OFs were pretreated with BBR (0, 1, 5, and 10 μM) for 12 hours and then incubated with TGF-β1 (10 ng/mL) for another 24 hours. HA concentrations in the supernatants were measured by ELISA, and *HAS1*, *HAS2*, and *HAS3* mRNA amounts were determined by qRT-PCR ($n = 3$). (**B**) *ACTA2*, *FN1*, *COL1A1*, and *COL3A1* mRNA amounts were detected upon incubation with TGF-β1 (10 ng/mL) for another 48 hours, $n = 6$. (**C**, **D**) The protein levels of fibrotic markers (α-SMA, fibronectin, collagen I, and collagen III) were evaluated upon incubation with TGF-β1 (10 ng/mL) for another 72 hours. (**E**) The bands of indicated proteins were quantified by densitometry ($n = 3$). Relative quantification was based on GADPH. $^{*}P < 0.05$, $^{**}P < 0.01$, $^{***}P < 0.001$, and $^{****}P < 0.0001$ versus control group; $^{\#}P < 0.05$, $^{\#\#}P < 0.01$, $^{\#\#\#}P < 0.001$, and $^{\#\#\#\#}P < 0.0001$ versus TGF-β1 group, one-way ANOVA.

Western blot data confirmed that the PPARγ and AMPK pathways both participated in the antiadipogenic effect exerted by BBR. Huang et al.[41] suggested that BBR inhibits adipocyte differentiation through the PPARγ pathway in adipocyte precursors (3T3-L1 cells). Previously reported findings demonstrated PPARγ and C/EBPα are not over-activated by C/EBPδ and C/EBPβ until the late stages of adipogenic differentiation,[42] which may explain the discrepancy between 5-day and 10-day mRNA expression levels (Figs. 1C, 1D). The remaining adipogenic proteins (FABP4, perilipin 1, adiponectin) suppressed by BBR are also downstream of the PPARγ pathway. Although BBR is

Investigative Ophthalmology & Visual Science

considered an AMPK activator for its upregulation of AMP in vivo and in vitro,[29,43] phosphorylation of AMPK (Thr172) is not always increased by BBR.[44] Gowans et al.[45] reported that allosteric activation of AMPK is a crucial component of the whole mechanism, which can enable BBR to enhance the downstream signaling pathways without Thr172 phosphorylation. Thus, combining these data with our findings, we deduce that BBR activates the AMPK pathway through allosteric activation and consequently suppresses the expression of SREBP and SCD1. This allosteric activation may also explain why compound C did not affect ERK phosphorylation in a previous study.[46] In conclusion, PPARγ inhibition and AMPK pathway activation both occur in the BBR-induced antiadipogenic effect in TAO OFs.

Proinflammatory cytokines, including IL-6 and COX-2, have been postulated as important mediators within the TAO orbit. Their exaggerated secretion is mainly attributed to the crosstalk among TSHR/IGF-IR, CD40–CD154, and IL-1R.[47,48] Our previous studies suggested PTX3 is a humoral immune molecule regulated by TSH and TGF-β in OFs and fibrocytes, and the upregulation can be blocked by IGF-IR inhibition.[23,24] In this research, gene expression and secreted protein amounts of IL-6, PTX3, and COX-2 were elevated by IL-1β treatment as expected. *IL-1*β mRNA was also robustly increased in an autocrine manner. We not only found IL-1β–induced expression of PTX3 in OFs but also confirmed that BBR inhibited this inflammatory cascade reaction by blocking the NF-κB pathway. It seems that BBR has a pervasive repression on the NF-κB pathway in both animals and cultured cells.[49–51] Additionally, HA production and myofibroblast differentiation elicited by TGF-β were significantly decreased by BBR treatment. HAS2 was identified as the primary contributor to HA production in the orbit.[52] BBR inhibited *HAS2* mRNA expression, which may explain the corresponding decline of HA accumulation. Despite the indicated mRNA expression levels being partly different between TAO and CON groups, levels of protein were close, and most tendencies treated by BBR were also consistent. Taken together, BBR attenuates inflammation, HA production, and fibrosis in both TAO-OFs and CON-OFs.

The gut microbiota recently surfaced as a novel contributor to TAO pathogenesis.[53] Besides the above effects, BBR also exerts great modulatory effects on the gut microbiota, as shown in patients with Graves' disease.[54] Regulating the gut microbiota and other in vivo activities of BBR should be conducted in future animal models of TAO. Second, several patients with TAO with GC treatment led to a limitation, even though over a 6-month gap existed before surgery. Last, the relevant effects of BBR on fibrocytes in peripheral blood and other immune cells remain unclear, which deserves further investigation.

Conclusion

In summary, given the prominent safety profile and affordable cost, the current data suggest that BBR is worth considering as a potent candidate for clinical trials to pharmaceutically alter TAO.

Acknowledgments

The authors thank the Department of Laboratory Medicine (Changzheng Hospital, Naval Medical University, Shanghai, China) for support with laboratory instruments and experimental techniques.

Supported by the National Natural Science Foundation of China (no. 81770959 and no. 81570885).

Disclosure: **J. Diao**, None; **X. Chen**, None; **P. Mou**, None; **X. Ma**, None; **R. Wei**, None

References

1. Smith TJ, Hegedus L. Graves' disease. *N Engl J Med.* 2016;375(16):1552–1565.
2. Wiersinga WM, Bartalena L. Epidemiology and prevention of Graves' ophthalmopathy. *Thyroid.* 2002;12(10):855–860.
3. Khoo TK, Coenen MJ, Schiefer AR, Kumar S, Bahn RS. Evidence for enhanced Thy-1 (CD90) expression in orbital fibroblasts of patients with Graves' ophthalmopathy. *Thyroid.* 2008;18(12):1291–1296.
4. Bahn RS. Thyrotropin receptor expression in orbital adipose/connective tissues from patients with thyroid-associated ophthalmopathy. *Thyroid.* 2002;12(3):193–195.
5. Smith TJ, Tsai CC, Shih MJ, et al. Unique attributes of orbital fibroblasts and global alterations in IGF-1 receptor signaling could explain thyroid-associated ophthalmopathy. *Thyroid.* 2008;18(9):983–988.
6. Lehmann GM, Feldon SE, Smith TJ, Phipps RP. Immune mechanisms in thyroid eye disease. *Thyroid.* 2008;18(9):959–965.
7. Galgoczi E, Jeney F, Gazdag A, et al. Cell density-dependent stimulation of PAI-1 and hyaluronan synthesis by TGF-beta in orbital fibroblasts. *J Endocrinol.* 2016;229(2):187–196.
8. Koumas L, Smith TJ, Feldon S, Blumberg N, Phipps RP. Thy-1 expression in human fibroblast subsets defines myofibroblastic or lipofibroblastic phenotypes. *Am J Pathol.* 2003;163(4):1291–1300.
9. Dik WA, Virakul S, van Steensel L. Current perspectives on the role of orbital fibroblasts in the pathogenesis of Graves' ophthalmopathy. *Exp Eye Res.* 2016;142:83–91.
10. Zang S, Ponto KA, Kahaly GJ. Clinical review: Intravenous glucocorticoids for Graves' orbitopathy: efficacy and morbidity. *J Clin Endocrinol Metab.* 2011;96(2):320–332.
11. Stan MN, Garrity JA, Carranza Leon BG, et al. Randomized controlled trial of rituximab in patients with Graves' orbitopathy. *J Clin Endocrinol Metab.* 2015;100(2):432–441.
12. Perez-Moreiras JV, Gomez-Reino JJ, Maneiro JR, et al. Efficacy of tocilizumab in patients with moderate-to-severe corticosteroid-resistant Graves orbitopathy: a randomized clinical trial. *Am J Ophthalmol.* 2018;195:181–190.
13. Douglas RS, Kahaly GJ, Patel A, et al. Teprotumumab for the treatment of active thyroid eye disease. *N Engl J Med.* 2020;382(4):341–352.
14. Men CJ, Kossler AL, Wester ST. Updates on the understanding and management of thyroid eye disease. *Ther Adv Ophthalmol.* 2021;13:25158414211027760.
15. Jin Y, Khadka DB, Cho WJ. Pharmacological effects of berberine and its derivatives: a patent update. *Expert Opin Ther Pat.* 2016;26(2):229–243.
16. Liang H, Wang Y. Berberine alleviates hepatic lipid accumulation by increasing ABCA1 through the protein kinase C delta pathway. *Biochem Biophys Res Commun.* 2018;498(3):473–480.
17. Payab M, Hasani-Ranjbar S, Baeeri M, et al. Development of a novel anti-obesity compound with inhibiting properties on the lipid accumulation in 3T3-L1 adipocytes. *Iran Biomed J.* 2020;24(3):155–163.
18. Chi L, Peng L, Pan N, Hu X, Zhang Y. The anti-atherogenic effects of berberine on foam cell formation are mediated

through the upregulation of sirtuin 1. *Int J Mol Med.* 2014;34(4):1087–1093.
19. Patti AM, Al-Rasadi K, Giglio RV, et al. Natural approaches in metabolic syndrome management. *Arch Med Sci.* 2018;14(2):422–441.
20. Ai F, Chen M, Yu B, et al. Berberine regulates proliferation, collagen synthesis and cytokine secretion of cardiac fibroblasts via AMPK-mTOR-p70S6K signaling pathway. *Int J Clin Exp Pathol.* 2015;8(10):12509–12516.
21. Choi CJ, Tao W, Doddapaneni R, et al. The effect of prostaglandin analogue bimatoprost on thyroid-associated orbitopathy. *Invest Ophthalmol Vis Sci.* 2018;59(15):5912–5923.
22. Sorisky A, Pardasani D, Gagnon A, Smith TJ. Evidence of adipocyte differentiation in human orbital fibroblasts in primary culture. *J Clin Endocrinol Metab.* 1996;81(9):3428–3431.
23. Wang H, Atkins SJ, Fernando R, Wei RL, Smith TJ. Pentraxin-3 is a TSH-inducible protein in human fibrocytes and orbital fibroblasts. *Endocrinology.* 2015;156(11):4336–4344.
24. Diao J, Chen X, Jiang L, Mou P, Wei R. Transforming growth factor-beta1 suppress pentraxin-3 in human orbital fibroblasts. *Endocrine.* 2020;70(1):78–84.
25. Zhang J, Tang H, Zhang Y, et al. Identification of suitable reference genes for quantitative RT-PCR during 3T3-L1 adipocyte differentiation. *Int J Mol Med.* 2014;33(5):1209–1218.
26. Imenshahidi M, Hosseinzadeh H. Berberis vulgaris and berberine: an update review. *Phytother Res.* 2016;30(11):1745–1764.
27. Brun RP, Kim JB, Hu E, Altiok S, Spiegelman BM. Adipocyte differentiation: a transcriptional regulatory cascade. *Curr Opin Cell Biol.* 1996;8(6):826–832.
28. Feng X, Sureda A, Jafari S, et al. Berberine in cardiovascular and metabolic diseases: from mechanisms to therapeutics. *Theranostics.* 2019;9(7):1923–1951.
29. Zhu X, Bian H, Wang L, et al. Berberine attenuates nonalcoholic hepatic steatosis through the AMPK-SREBP-1c-SCD1 pathway. *Free Radic Biol Med.* 2019;141:192–204.
30. Jeong HW, Hsu KC, Lee JW, et al. Berberine suppresses proinflammatory responses through AMPK activation in macrophages. *Am J Physiol Endocrinol Metab.* 2009;296(4):E955–964.
31. Neag EJ, Smith TJ. 2021 update on thyroid-associated ophthalmopathy. *J Endocrinol Invest.* 2022;45(2):235–259.
32. Mercurio F, Manning AM. Multiple signals converging on NF-kappaB. *Curr Opin Cell Biol.* 1999;11(2):226–232.
33. Bahn RS. Graves' ophthalmopathy. *N Engl J Med.* 2010;362(8):726–738.
34. Liu X, Wang L, Tan S, et al. Therapeutic effects of berberine on liver fibrosis are associated with lipid metabolism and intestinal flora. *Front Pharmacol.* 2022;13:814871.
35. Zhu Y, Xie N, Chai Y, et al. Apoptosis induction, a sharp edge of berberine to exert anti-cancer effects, focus on breast, lung, and liver cancer. *Front Pharmacol.* 2022;13:803717.
36. Liu CS, Zheng YR, Zhang YF, Long XY. Research progress on berberine with a special focus on its oral bioavailability. *Fitoterapia.* 2016;109:274–282.
37. Dolman PJ. Evaluating Graves' orbitopathy. *Best Pract Res Clin Endocrinol Metab.* 2012;26(3):229–248.
38. Wang X, Yang S, Ye H, et al. Disulfiram exerts antiadipogenic, anti-inflammatory, and antifibrotic therapeutic effects in an in vitro model of Graves' orbitopathy. *Thyroid.* 2022;32(3):294–305.
39. Tao W, Ayala-Haedo JA, Field MG, Pelaez D, Wester ST. RNA-sequencing gene expression profiling of orbital adipose-derived stem cell population implicate HOX genes and WNT signaling dysregulation in the pathogenesis of thyroid-associated orbitopathy. *Invest Ophthalmol Vis Sci.* 2017;58(14):6146–6158.
40. Lee JY, Gallo RA, Ledon PJ, et al. Integrating differential gene expression analysis with perturbagen-response signatures may identify novel therapies for thyroid-associated orbitopathy. *Transl Vis Sci Technol.* 2020;9(9):39.
41. Huang C, Zhang Y, Gong Z, et al. Berberine inhibits 3T3-L1 adipocyte differentiation through the PPARgamma pathway. *Biochem Biophys Res Commun.* 2006;348(2):571–578.
42. Yeh WC, Cao Z, Classon M, McKnight SL. Cascade regulation of terminal adipocyte differentiation by three members of the C/EBP family of leucine zipper proteins. *Genes Dev.* 1995;9(2):168–181.
43. Zhang Y, Ye J. Mitochondrial inhibitor as a new class of insulin sensitizer. *Acta Pharmaceutica Sinica. B.* 2012;2(4):341–349.
44. Choi JS, Kim JH, Ali MY, et al. Anti-adipogenic effect of epiberberine is mediated by regulation of the Raf/MEK1/2/ERK1/2 and AMPKα/Akt pathways. *Arch Pharm Res.* 2015;38(12):2153–2162.
45. Gowans GJ, Hawley SA, Ross FA, Hardie DG. AMP is a true physiological regulator of AMP-activated protein kinase by both allosteric activation and enhancing net phosphorylation. *Cell Metab.* 2013;18(4):556–566.
46. Han YE, Hwang S, Kim JH, et al. Biguanides metformin and phenformin generate therapeutic effects via AMP-activated protein kinase/extracellular-regulated kinase pathways in an in vitro model of Graves' orbitopathy. *Thyroid.* 2018;28(4):528–536.
47. Hwang CJ, Afifiyan N, Sand D, et al. Orbital fibroblasts from patients with thyroid-associated ophthalmopathy overexpress CD40: CD154 hyperinduces IL-6, IL-8, and MCP-1. *Invest Ophthalmol Vis Sci.* 2009;50(5):2262–2268.
48. Li B, Smith TJ. Regulation of IL-1 receptor antagonist by TSH in fibrocytes and orbital fibroblasts. *J Clin Endocrinol Metab.* 2014;99(4):E625–E633.
49. Hsiang CY, Wu SL, Cheng SE, Ho TY. Acetaldehyde-induced interleukin-1beta and tumor necrosis factor-alpha production is inhibited by berberine through nuclear factor-kappaB signaling pathway in HepG2 cells. *J Biomed Sci.* 2005;12(5):791–801.
50. Wang Y, Huang Y, Lam KS, et al. Berberine prevents hyperglycemia-induced endothelial injury and enhances vasodilatation via adenosine monophosphate-activated protein kinase and endothelial nitric oxide synthase. *Cardiovasc Res.* 2009;82(3):484–492.
51. Jin BR, An HJ. Oral administration of berberine represses macrophage activation-associated benign prostatic hyperplasia: a pivotal involvement of the NF-κB. *Aging (Albany NY).* 2021;13(16):20016–20028.
52. Zhang L, Bowen T, Grennan-Jones F, et al. Thyrotropin receptor activation increases hyaluronan production in preadipocyte fibroblasts: contributory role in hyaluronan accumulation in thyroid dysfunction. *J Biol Chem.* 2009;284(39):26447–26455.
53. Wang Y, Ma XM, Wang X, et al. Emerging insights into the role of epigenetics and gut microbiome in the pathogenesis of Graves' ophthalmopathy. *Front Endocrinol (Lausanne).* 2021;12:788535.
54. Han Z, Cen C, Ou Q, et al. The potential prebiotic berberine combined with methimazole improved the therapeutic effect of Graves' disease patients through regulating the intestinal microbiome. *Frontiers in Immunology.* 2021;12:826067.

Investigative Ophthalmology & Visual Science